A predictive control framework for optimal energy extraction of wind farms

Vali, M.; Van Wingerden, J. W.; Boersma, S.; Petrović, V.; Kühn, M.

Important note
To cite this publication, please use the final published version (if applicable).
Please check the document version above.

A predictive control framework for optimal energy extraction of wind farms

A predictive control framework for optimal energy extraction of wind farms

M. Vali[1], J.W. van Wingerden[2], S. Boersma[2], V. Petrović[1] and M. Kühn[1]

[1] ForWind, University of Oldenburg, Institute of Physics, Küpkersweg 70, 26129 Oldenburg, Germany.
[2] Delft Center of Systems and Control, Delft University of Technology, Mekelweg 2, 2628 CD Delft, The Netherlands.

E-mail: `mehdi.vali@uni-oldenburg.de`

Abstract. This paper proposes an adjoint-based model predictive control for optimal energy extraction of wind farms. It employs the axial induction factor of wind turbines to influence their aerodynamic interactions through the wake. The performance index is defined here as the total power production of the wind farm over a finite prediction horizon. A medium-fidelity wind farm model is utilized to predict the inflow propagation in advance. The adjoint method is employed to solve the formulated optimization problem in a cost effective way and the first part of the optimal solution is implemented over the control horizon. This procedure is repeated at the next controller sample time providing the feedback into the optimization. The effectiveness and some key features of the proposed approach are studied for a two turbine test case through simulations.

1. Introduction

Control of turbines in a wind farm is challenging because of the aerodynamic interactions via wakes. The characteristics of a wake are reduced wind speed and increased turbulence. The former reduces the total power production of the farm and the latter leads to a higher dynamic loading on the downstream turbines. Thus, in order to lower the levelized cost of energy by wind farm control the two main objectives are minimizing the wake-induced power losses and structural fatigue loads, e.g. by optimizing the individual wind turbine control settings [1].

Several studies have utilized optimization techniques to find the optimal set-points for the total wind farm performance [2-5]. Campagnolo *et al.* [6] have investigated the potential of different wind farm control strategies through wind tunnel testing. Nonetheless, from a control design perspective, the approaches followed so far have been open-loop ones while the inherent modeling uncertainties and time-varying inflow conditions, e.g. wind direction changes and wake meandering, demand for a dynamic closed-loop approach.

Soleimanzadeh *et al.* [7] have developed a linear state-space model and a distributed controller for the wind farm which is only valid for really small deviations from the equilibrium. Goit *et al.* [8] have proposed an optimal control of energy extraction, utilizing Large Eddy Simulation (LES) model and optimal control theory [9] to increase the turbulent kinetic energy of inflow within a wind farm. The proposed controller relies on a full high-fidelity LES model to compute the optimal control commands, which is time consuming for real-time control. However, a control-oriented model should capture all dominant inflow dynamics in a computationally inexpensive manner. This is the main motivation of studying medium-fidelity models for wind farms [10-14].

In this paper an adjoint-based model predictive control (AMPC) framework is developed for wind farms using WindFarmSimulator (WFSim), a control-oriented dynamic medium-fidelity wind farm model [13,14]. The wind farm control target here is to react against the low-frequency wake-induced power losses and loads, i.e. in the order of one minute. To reach this goal, a constrained optimization problem is formulated, which considers the aerodynamic interactions of the wind turbines through wakes. The performance index is specified here to maximize the power production of a farm, which can be extended to optimal load distribution as well. We exploit the discrete adjoint approach to obtain the gradient of the specified performance index at a finite prediction horizon. The adjoint field reveals which turbine at which time can contribute to maximization of the total power. Then, similar to [8], we employ a nonlinear conjugate gradient method for solving the optimization problem due to its computational effectiveness. Here, we solve the problem with respect to the axial induction factor of the wind turbines, which can be extended to the yaw control as well. At the end, we evaluate and discuss the performance of the AMPC for two different wind farm operating points with full and partial wake interactions.

The remainder of this paper is organized as follows. In section 2, we present briefly the fundamentals of WFSim. Section 3 focuses on the structure of the proposed AMPC for wind farm control, including the formulated constrained optimization problem, the adjoint-based gradient of the performance index and the optimization method. The previously explained method is studied in section 4 for a relatively simple two turbine case through simulations. Finally, the conclusions of this paper are collected in section 5.

2. Wind Farm model

This section presents briefly the fundamentals of the WFSim, a control-oriented dynamic medium-fidelity wind farm model [13,14]. An important feature of the WFSim is the sparsity in the system matrices, improving the computational efficiency. The wind flow is modeled using the 2D Navier Stokes equations constrained by the continuity equation [16]:

$$\rho \frac{\partial u}{\partial t} + \rho \nabla (u\mathbf{u}) = -\frac{\partial p}{\partial x} + \nabla (\mu \nabla u) + S_x + T_x, \tag{1}$$

$$\rho \frac{\partial v}{\partial t} + \rho \nabla (v\mathbf{u}) = -\frac{\partial p}{\partial y} + \nabla (\mu \nabla v), \tag{2}$$

$$\rho \nabla (\mathbf{u}) = 0. \tag{3}$$

where ρ is the air density, μ is the viscosity, p is the pressure field and $\mathbf{u} = [u, v]$ is the velocity vector field. S_x represents the external source terms in the x direction, employed for incorporating the wind turbine models. The term T_x represents the turbulence model, which is the mixing length model in WFSim [14]. The set of equations (1)-(3) are spatially discretized, using the Hybrid differencing scheme, over a staggered grid of $(N_x \times N_y)$ cells. Furthermore, the backward differencing scheme is employed to discretize the flow model temporally for the unsteady solution [10,13].

A wind turbine is modeled using the actuator disc theory to exert a thrust force into the incoming flow and extract a certain amount of power from the wind. The thrust force for the ith turbine in a wind farm is expressed as follows [17]

$$F_{T_i} = \frac{1}{2} \rho A_d U_\infty^2 C_T(a_i), \qquad C_T(a_i) = 4a_i(1 - a_i). \tag{4}$$

where U_∞ is the effective wind speed at far distance upwind the rotor, A_d the swept area of the rotor plane, and C_T is the thrust coefficient of the turbine which is a function of the axial induction factor a_i. The latter is a measure of the decrease in the stream-wise flow velocity at the rotor plane.

Considering the induction effect of the rotor disc as $U_d = (1 - a)U_\infty$ enables us to estimate the exerted thrust force using the measurable wind velocity U_d at the rotor and the axial induction factor. Therefore, the ith turbine model is incorporated inside the flow model (1) as follows

$$S_{x_i} = F_{T_i} = \underbrace{2\rho A_d U_{d_i}^2}_{B_{x_i}} \beta_i, \qquad \beta_i = \frac{a_i}{1 - a_i}, \tag{5}$$

where the virtual control variable β_i is defined to obtain a linear expression of the thrust force with respect to the wind turbine control setting [13]. Furthermore, the induction factor a_i is combined with a first order lag to model the wind turbine dynamic inflow as follows

$$\dot{a}_i = \frac{1}{\tau}(a_{i,c} - a_i), \tag{6}$$

where $a_{i,c}$ is the ith wind turbine control command and τ represents the aerodynamic time constant, which is approximated by $\tau = 13.5\,\text{s}$ [22].

Finally, the wind farm model over the specified staggered grid can be given in matrix form as follows [13]

$$\underbrace{\begin{bmatrix} A_x(\bar{u}_k, \bar{v}_k) & 0 & B_1 \\ 0 & A_y(\bar{u}_k, \bar{v}_k) & B_2 \\ B_1^T & B_2^T & 0 \end{bmatrix}}_{A(X_k)} \begin{bmatrix} \bar{u}_{k+1} \\ \bar{v}_{k+1} \\ \bar{p}_{k+1} \end{bmatrix} = \underbrace{\begin{bmatrix} c_x & 0 & 0 \\ 0 & c_y & 0 \\ 0 & 0 & 0 \end{bmatrix}}_{Q} \begin{bmatrix} \bar{u}_k \\ \bar{v}_k \\ \bar{p}_k \end{bmatrix} + \underbrace{\begin{bmatrix} B_x(\bar{u}_k) \\ 0 \\ 0 \end{bmatrix}}_{B(X_k)} \beta_k + \underbrace{\begin{bmatrix} b_x(\bar{u}_k, \bar{v}_k) \\ b_y(\bar{u}_k, \bar{v}_k) \\ b_c \end{bmatrix}}_{b(X_k)}. \tag{7}$$

where $\bar{u}_k \in \mathbb{R}^{(N_x-3)(N_y-2)\times 1}$, $\bar{v}_k \in \mathbb{R}^{(N_x-2)(N_y-3)\times 1}$ and $\bar{p}_k \in \mathbb{R}^{(N_x-2)(N_y-2)\times 1}$ are the vectors that stack all the velocities and pressures in every point of the staggered grid at the time instant k. By defining $X = [\bar{u}, \bar{v}, \bar{p}]^T$, the matrix $A(X_k)$ represents the spatial discretization terms of the x and y-momentum and the continuity equations (1)-(3). The constant matrix Q is referred to the temporal discretization of the flow depending on the chosen sampling time and the matrix $B(X_k)$ represents the linear expession of the thrust force with respect to the virtual control input β_k. Finally the matrix $b(X_k)$ represents the effect of the zero-gradient boundary conditions. The reader is referred to [13,14] for more details on the 2D wind farm model.

3. Optimal control of energy extraction
In this section, an adjoint-based model predictive control (AMPC) framework is proposed for wind farms. MPC is an optimal control technique employing real-time optimization. The control inputs and plant responses are predicted in advance and optimized for finite time intervals, the so called prediction horizon, with respect to a performance index. Then, the first part of the optimal solution, depending on the controller sample time, is applied to the system. This procedure is repeated in the next controller sample time which provides the feedback into the optimization.

Figure 1 demonstrates schematically the proposed framework for the adjoint-based model predictive control (AMPC). It contains three main steps: prediction, solving an optimization problem over a finite time prediction horizon N_p and implementing the optimal control solutions over the receding time horizon $N_u \le N_p$. Optimality is in this paper defined as the maximum power that can be extracted by a given wind farm over a specified time horizon using the axial induction factor a_i, for $i = 1, 2, \ldots, N_t$ with N_t the number of turbines. Similar to [8], we exploit the adjoint approach as an effective tool to speed up the computation of the gradient of the performance index. In the proposed framework, the optimization problem can be extended to other performance indices, e.g. wind farm power demand tracking or optimal load distribution on the wind turbines. Furthermore, the optimization variables can be considered as the practical wind turbine control settings, e.g. pitch, rotor speed and yaw control.

The predictive control approximates in advance the inflow propagation within a farm over the finite prediction horizon N_p (see blue arrow in Fig. 1). It utilizes WFSim to predict the two dimensional velocity vector field of the flow [13,14]. The flow estimations can be improved using the ensemble Kalman filter [15].

Then, the adjoint field corresponding to the predicted flow (see red arrow in Fig. 1) is computed. The adjoint field which propagates backward depends strongly on the predicted flow and the definition
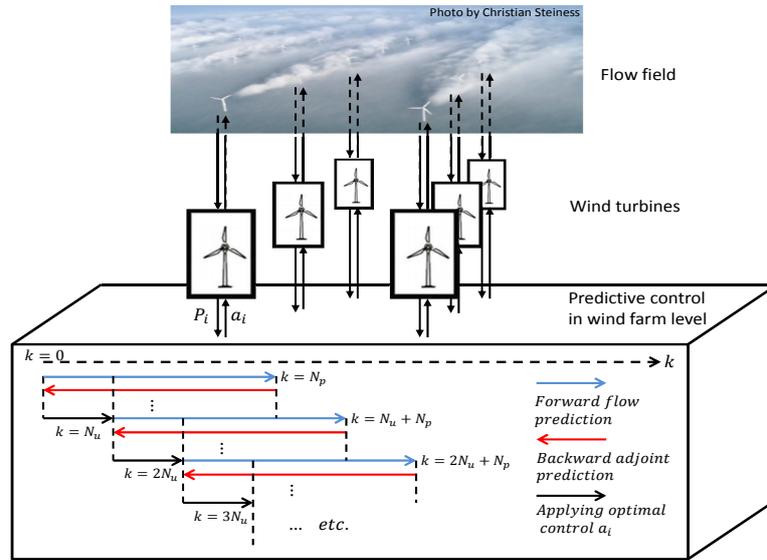
Figure 1: Schematic illustration of the adjoint-based model predictive control (AMPC) of wind farms

of the performance index [8]. It is utilized as a cost-effective tool to compute the gradient of the cost function with respect to the wind turbine control settings. Then, the formulated optimization problem is solved, employing a nonlinear conjugate-gradient method combined with a line search method. Finally, the optimal solution, i.e. the axial induction factor, is implemented at the receding time horizon N_u (see black arrow in Fig. 1). The whole procedure is repeated for the next receding horizon N_u, which incorporates feedback inside the optimization. The reader is referred to [18] for more details on the nonlinear model predictive control. In the following sections, the details of the proposed AMPC for optimal energy extraction of wind farms are explained.

3.1. Energy extraction of a single wind turbine
According to the actuator disc theory [17], the power production of a single turbine is defined as

$$P = \frac{1}{2}\rho A_d U_\infty^3 C_P(a), \qquad C_P(a) = 4a(1-a)^2. \tag{8}$$

where C_P is the power coefficient of the wind turbine with dependency on the axial induction factor. The effective wind speed U_∞ at infinite distance upwind the rotor is estimated using the measurable wind velocity U_d at grid cells in which the rotor disc is located as follows [17]

$$\hat{U}_\infty = \frac{C_f(a)U_d}{1-a}, \tag{9}$$

where the correction factor $C_f(a)$ is defined empirically to make the approximation more precise ($\hat{U}_\infty - U_\infty \approx 0$). The power production of a single turbine simulated in WFSim is validated with the actuator disc theory. Figure 2 shows the power coefficient of a single turbine compared with (8). The necessity of the correction factor $C_f(a)$ in modeling a wind turbine as an actuator disc is illustrated as well. Note that the power coefficient of the implemented wind turbine in WFSim is obtained by substituting (9) into (8) yielding

$$C_P(a) = \frac{P}{\frac{1}{2}\rho A_d U_\infty^3} = \frac{4a}{1-a}\left(\frac{C_f(a)U_d}{U_\infty}\right)^3. \tag{10}$$

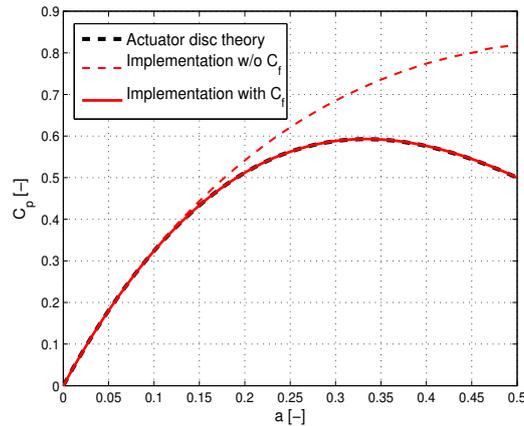where U_d is the rotor averaged inflow velocity computed by WFSim.

Figure 2: Energy extraction of a single turbine simulated in WFSim (10), compared with the actuator disc theory (8)

3.2. Optimization problem formulation

This section focuses on the optimization problem which is solved in our predictive control framework for optimal energy extraction of wind farms. The optimization variables are the wind turbine control parameters at time instant k as $\beta_k = [\beta_{1,k}, \beta_{2,k}, \ldots, \beta_{N_t,k}]^T \in \mathbb{R}^{N_t \times 1}$. Note that we formulate the problem with respect to the virtual variable $\beta_i = \frac{a_i}{1-a_i}$ such that we have a linear expression of the thrust force with respect to the control input. The state variable at time instant k is $X_k = [\bar{u}_k, \bar{v}_k, \bar{p}_k]^T$ as defined in (7).

The optimal control problem is formulated as finding the maximum power production of the wind farm over a finite time horizon N_p. Hence, we first define the following performance index, referring to the total power production, at each time instant k as follows

$$\mathscr{J}_k(X_k, \beta_k) = -\sum_{i=1}^{N_t} P_{i,k} \tag{11}$$

Now, we can formulate the following constrained optimization problem over the prediction time horizon N_p

$$\min_{\tilde{\beta}} \quad \mathscr{J}(\tilde{X}, \tilde{\beta}) = \sum_{k=1}^{N_p} \mathscr{J}_k(X_k, \beta_k), \tag{12}$$

$$\text{s.t.} \quad \tilde{\mathbf{C}}(\tilde{X}, \tilde{\beta}) = 0, \tag{13}$$

$$0 \leq \beta_{i,k} \leq 1. \tag{14}$$

The equality constraint (13) represents the spatial and temporal discretized inflow model, evolving over the prediction horizon time N_p with the following expanded form

$$\tilde{\mathbf{C}} = \begin{bmatrix} C_1(X_0, X_1, \beta_0) \\ C_2(X_1, X_2, \beta_1) \\ \vdots \\ C_{N_p}(X_{N_p-1}, X_{N_p}, \beta_{N_p-1}) \end{bmatrix}, \quad \tilde{X} = \begin{bmatrix} X_1 \\ X_2 \\ \vdots \\ X_{N_p} \end{bmatrix}, \quad \tilde{\beta} = \begin{bmatrix} \beta_1 \\ \beta_2 \\ \vdots \\ \beta_{N_p} \end{bmatrix},$$

where according to (7)

$$C_k(X_{k-1}, X_k, \beta_{k-1}) = A(X_{k-1})X_k - QX_{k-1} - B(X_{k-1})\beta_{k-1} - b(X_{k-1}) = 0. \tag{15}$$

Furthermore, the inequality constraint (14) refers to the constraints on the wind turbine control input.

To improve the performance, a gradient-based optimization method is performed to solve the formulated problem (12)-(14) with the search directions, defined by the gradient of the performance index at the current state of each prediction window. This is the main focus of the following sections.

3.3. Adjoint-based gradient of the cost function

Adjoint methods give an efficient way to obtain the gradient of a performance index, when having many decision variables. We utilize the discrete adjoint approach to obtain accurate derivatives of the performance index, because it avoids the error-prone and tedious derivation and discretization of the continuous one [19].

First, we define the *Lagrangian* to turn the constrained optimization problem (12)-(13) into the unconstrained one as follows

$$\mathscr{L}(\tilde{X},\tilde{\beta},\Lambda) \equiv \mathscr{J}(\tilde{X},\tilde{\beta}) + \Lambda^T \tilde{\mathbf{C}}(\tilde{X},\tilde{\beta}), \tag{16}$$

where in this context Λ is the vector of *Lagrange multipliers* over the finite time horizon in which we optimize and equation $\tilde{\mathbf{C}}(\tilde{X},\tilde{\beta}) = 0$ represents the constraint on the dynamic optimization problem, i.e. the wind farm model. Since this constraint holds everywhere for $k = 1, 2, \cdots, N_p$, we may choose Λ freely yielding

$$\mathscr{L}(\tilde{X},\tilde{\beta},\Lambda) = \mathscr{J}(\tilde{X},\tilde{\beta}). \tag{17}$$

Hence, the gradient of the cost function can be obtained as follows

$$\nabla_{\tilde{\beta}}\mathscr{J} = (\mathscr{J}_{\tilde{X}} + \Lambda^T \tilde{\mathbf{C}}_{\tilde{X}})\tilde{X}_{\tilde{\beta}} + \mathscr{J}_{\tilde{\beta}} + \Lambda^T \tilde{\mathbf{C}}_{\tilde{\beta}}, \tag{18}$$

where $(.)_{\tilde{X}}$ and $(.)_{\tilde{\beta}}$ represent the partial derivatives with respect to the $\tilde{X}$ and $\tilde{\beta}$, respectively.

Recalling wind farm model (7), it is assumed that for all allowable control setting β_k, our discretized model has a unique solution X_{k+1}. Now one may define the adjoint field Λ over the specified time horizon N_p as a solution of the adjoint equation [19]

$$\tilde{\mathbf{C}}_{\tilde{X}}^T(\tilde{X},\tilde{\beta})\Lambda = -\mathscr{J}_{\tilde{X}}^T(\tilde{X},\tilde{\beta}) \tag{19}$$

where

$$\tilde{\mathbf{C}}_{\tilde{X}} = \begin{bmatrix} (C_1)_{X_1} & 0 & \cdots & 0 & 0 \\ (C_2)_{X_1} & (C_2)_{X_2} & \cdots & 0 & 0 \\ \vdots & \ddots & \ddots & \vdots & \vdots \\ 0 & 0 & \ddots & (C_{N_p-1})_{X_{N_p-1}} & 0 \\ 0 & 0 & \cdots & (C_{N_p})_{X_{N_p-1}} & (C_{N_p})_{X_{N_p}} \end{bmatrix}, \tag{20}$$

with the linearized components of the wind farm model (15) as

$$\begin{aligned} (C_k)_{X_k} &= A(X_{k-1}), \\ (C_k)_{X_{k-1}} &= (A(X_{k-1})X_k)_{X_{k-1}} - Q - (B(X_{k-1})\beta_{k-1})_{X_{k-1}} - (b(X_{k-1}))_{X_{k-1}}. \end{aligned} \tag{21}$$

The reader is referred to [14] for more details on the linearized model. Expanding adjoint equation (19) yields the propagation of the adjoint field backward over the time horizon N_p, i.e. $\Lambda = [\lambda_1, \lambda_2, \cdots, \lambda_{N_p}]^T$, as follows

$$(C_{k-1})_{X_{k-1}}^T \lambda_{k-1} = -\mathscr{J}_{X_{k-1}}^T(\tilde{X},\tilde{\beta}) - (C_k)_{X_{k-1}}^T \lambda_k. \tag{22}$$

with initializing $\lambda_{N_p+1} = 0$. The structure of the adjoint equation (19) indicates that the adjoint field is obtained based on the definition of the performance index $\mathscr{J}$ and the wind farm model. It propagates backward and indicates the temporal and spatial influences of the wind turbines, through their control settings, on the wind farm power production. Therefore, it is a useful tool to obtain a search direction, yielding the improvement in the performance.

By substituting the adjoint field Λ into (18), there is no need for tedious calculation of the derivatives of the flow solution with respect to the control variables ($\tilde{X}_{\tilde{\beta}}$) over the prediction horizon. Finally, the

gradient of the cost function (12), $\nabla_{\tilde{\beta}}\mathscr{J} = [\nabla_{\beta_1}\mathscr{J}, \nabla_{\beta_2}\mathscr{J}, ..., \nabla_{\beta_{N_p}}\mathscr{J}] \in \mathbb{R}^{1 \times N_t N_p}$, can be expressed in compact form as follows

$$\nabla_{\tilde{\beta}}\mathscr{J} = \mathscr{J}_{\tilde{\beta}}(\tilde{X}, \tilde{\beta}) + \Lambda^T \tilde{\mathbf{C}}_{\tilde{\beta}}(\tilde{X}, \tilde{\beta}), \tag{23}$$

Exploiting the sparse structure of the matrix $\tilde{\mathbf{C}}_{\tilde{\beta}}$, similar to (19), yields the time-dependency of the gradient $\nabla_{\beta_{k-1}}\mathscr{J} \in \mathbb{R}^{1 \times N_t}$ at the horizon in which we maximize the power extraction of the wind farm as

$$\nabla_{\beta_{k-1}}\mathscr{J} = \mathscr{J}_{\beta_{k-1}}(\tilde{X}, \tilde{\beta}) - \lambda_k^T B(X_{k-1}). \tag{24}$$

3.4. Optimization method

This section briefly introduces the employed nonlinear conjugate gradient optimization method for solving the formulated problem (12)-(14). Conjugate gradient methods are efficient approaches when the number of optimization variables is large due to the employment of a few vector operations.

Given an estimated control variables $\tilde{\beta}^{(n)} \in \mathbb{R}^{N_t N_p \times 1}$ at the nth optimization iteration, a search direction $\delta\tilde{\beta}^{(n)}$ is obtained using the conjugate gradient method as follows

$$\delta\tilde{\beta}^{(n)} = -\nabla_{\tilde{\beta}}\mathscr{J}^{(n)} + \eta^{(n)}\delta\tilde{\beta}^{(n-1)}. \tag{25}$$

where $\nabla_{\tilde{\beta}}\mathscr{J}$ is the adjoint-based gradient of the cost function over the finite time horizon N_p determined by (24). The parameter η is a characteristic for the optimization method which guarantees the proper calculation of search direction. Similar to [8], we utilize the Polak-Ribière method [20] at each iteration. The obtained search direction $\delta\tilde{\beta}^{(n)}$ is used to estimate a new set of optimal control variables for the next iteration. Moreover, a backtracking line search based on the Armijo rule [21] is employed to search iteratively the best feasible improvement in the total power production along with the search direction, considering the practical constraint on the wind turbines control input.

4. Simulation studies

The performance of the adjoint-based predictive wind farm controller is analyzed here through simulation studies with WFSim. A simple example of two turbines in a row is considered. The wind turbines with rotor diameter $D = 126$ m are spaced $5D$ in the stream-wise direction. We have a field of 2000×1000 m^2 with a staggered grid of 100×50 cells ($N_x \times N_y$). Figure 3 depicts our example operating at ambient wind speed $U_\infty = 10$ m/s for two different wind farm operating conditions, i.e. the full wake (left) and the partial wake (right) interactions. Here, the flow is simulated for laminar flow conditions, where viscous forces are dominant. The performance of the AMPC is analyzed here for atmospheric conditions without changing the incoming flow, compared with the greedy control setting ($a_i = \frac{1}{3}$).
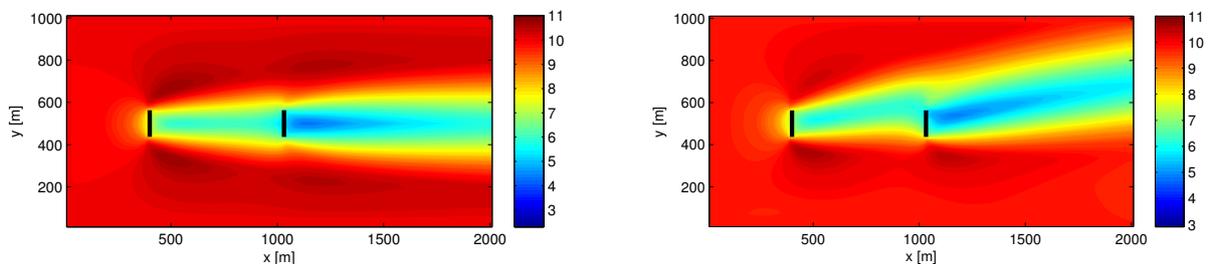

Figure 3: Two-turbine example with $U_\infty = 10$ m/s, simulated in WFSim. (left) The incoming flow aligned to the rotor discs, resulting full wake interactions. (right) The wind direction is misaligned $10°$ with the rotor discs, resulting partial wake interactions.

4.1. Grid search for optimal solution

In order to find the optimal control settings of two turbines in a row as a reference, a grid search procedure is employed for the steady state solution of the WFSim, with $U_\infty = 10$ m/s for the full wake interactions (see left image of Fig. 3). A two-dimensional grid is constructed with respect to the axial induction factor of each turbine, which becomes dense around the pre-guessed optimal solutions. Note that the incoming flow is simulated aligned to the rotor discs for all cases. Figure 4 illustrates the contour plot of the resulting total power, which is normalized with respect to the maximum amount of the achieved power, for all possible combinations of the control settings. For our simulated example, grid search approach finds the local optimal solution $a_{\text{opt}} = [0.225, 0.305]$. Therefore, assuming the atmospheric conditions remain stable, the power production might increase 3.87%, compared with the greedy wind turbine control setting ($a_i = 0.33$). The small reduction in the induction factor of the downwind turbine might be attributed to its minor aerodynamic influence on the upwind one due to the turbines spacing and flow specifications of our simulation example.
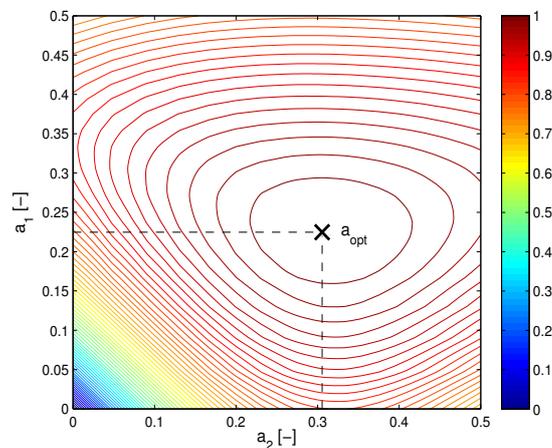

Figure 4: The contour plot of the total power with $U_\infty = 10$ m/s. The achieved optimal solution is $a_{\text{opt}} = [0.225, 0.305]$. The power outputs are normalized with respect to the maximum amount of the achieved power.

4.2. Performance of adjoint-based model predictive control (AMPC)

In this section we evaluate the performance of the proposed control framework under atmospheric conditions without changing the incoming flow. The wind farm starts operating with the greedy control setting $a_i = 0.33$, at the ambient wind speed 10 m/s. After inflow propagation and wake interactions, the AMPC is activated at time instant 1000 s. Here, we investigate two simulation scenarios: the first full wake interactions, while the inflow is aligned to the rotor discs (see left image of Fig. 3) and the second partial wake interactions, when inflow is misaligned 10° to the rotors (see left image of Fig. 3). Furthermore, we show the performance with the optimal control settings obtained through the offline grid search for the case study 1, i.e. full wake interactions. The aim is to illustrate the necessity of the dynamic closed-loop control for different wind farm operating points.

4.2.1. Case study 1: Full wake interactions

Here, the rotor discs are aligned with the wind direction to evaluate the performance of the AMPC whilst both wind turbines are interacting fully through wakes (see left image of Fig. 3). Figure 5 shows the optimal control of the energy extraction for our example, compared with the greedy control. Moreover, the total power production of the wind turbines operating with the grid search optimal solution $a_{\text{opt}} = [0.225, 0.305]$ is also shown as a reference.

The AMPC maximizes the total power of the wind farm dynamically to the same level of the grid search solution. Note that the optimal solution of the grid search is valid only for the stationary
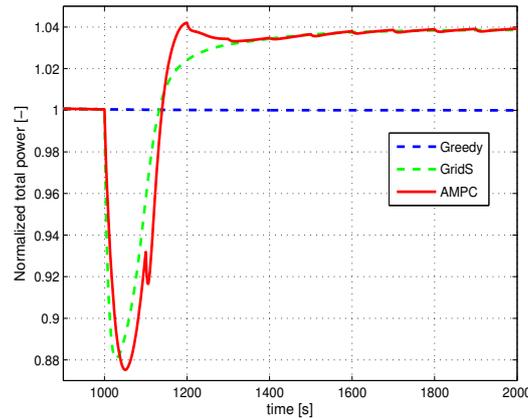
Figure 5: Total power production with fully wake interactions, normalized with respect to the case with the greedy control setting. (prediction horizon $N_p = 600\,$s, control horizon $N_u = 100\,$s).
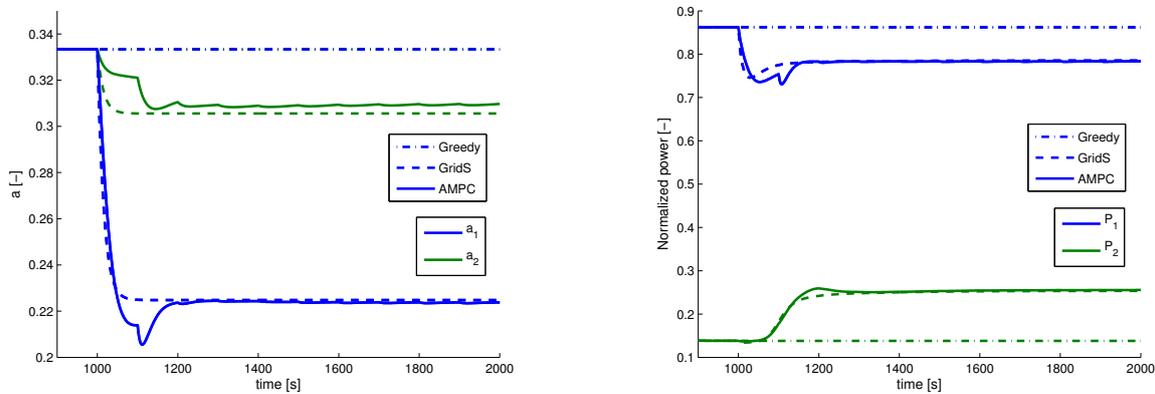

Figure 6: (left) The induction factor and (right) the power production of the individual wind turbines for different simulation cases, with ambient wind $U_\infty = 10\,$m/s. The power production is normalized with respect to the total power of the greedy control.

atmospheric conditions. After complete convergence, simulation results show that the AMPC can increase the total power by 3.87% for our simulated example, compared with the greedy control.

Figure 6 illustrates the time-varying behaviour of the axial induction factor (left) and the corresponding power production (right) of each turbine. It can be seen that the AMPC reduces the energy extraction of the upwind turbine to increase the kinetic energy of the inflow reaching the downstream turbine. The downwind turbine performs almost at the greedy control setting to capture the most possible energy from the incoming wind. The induced optimal induction factors almost converge to the grid search solution, computed offline for this specific atmospheric condition. The existing discrepancy might be related to the small errors in the computation of the gradient or the relatively large tolerances, determined to keep the optimization computationally inexpensive.

4.2.2. Case study 2: Partial wake interactions A rotor disc must precisely face the wind to deliver its maximum power output. However, wind turbines might be misaligned in reality due to the wind direction sensor inaccuracies or delay in the wind direction tracking. Yaw misalignment results in both wind turbine power losses and additional dynamic loads. In the wind farm level, yaw misalignment of the upwind turbine can redirect its wake downstream and consequently affect the performance of the downwind turbine. We investigate here the performance of the AMPC while the inflow direction is misaligned $10°$ with respect to the rotor discs (see right image of Fig. 3). The main goal here is to assess the performance of the proposed approach in a different operating condition.

Figure 7 shows the total power production for our example with 10° yaw misalignment, operating with different control strategies. The power outputs are normalized with respect to the total power of the greedy control setting with full wake interactions (see Fig. 5). Note that the total power production is increased here due to the upwind turbine misalignment, which tends to redirect its own wake away from the downwind turbine. In other words, the turbines interactions through wakes are reduced and more kinetic energy reaches the downstream turbine, compared with the case study 1.

As expected, the obtained optimal control setting $a_{\text{opt}} = [0.225, 0.305]$ would not be advantageous anymore for this new wind farm operating condition (green dashed plot). Compared with the greedy control setting, the power gain of the downstream turbine is almost the same as the power loss of the upwind turbine. This control setting might be interesting in optimal load distribution, which is out of the focus of this paper. Nonetheless, it can be seen that the AMPC is capable of maximizing the energy extraction of the wind farm dynamically in this new operating wake condition.
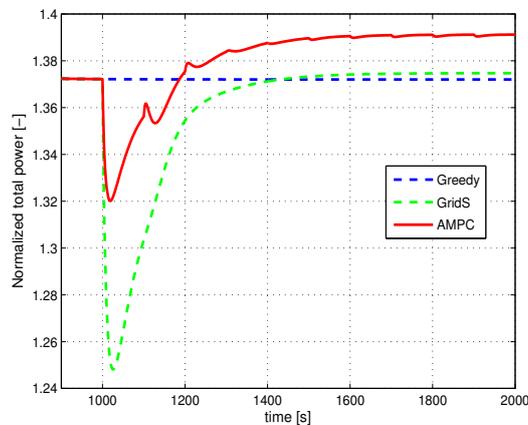

Figure 7: Total power production with 10° yaw misalignment, normalized with respect to the greedy control setting with fully wake interactions. (prediction horizon $N_p = 600$ s, control horizon $N_u = 100$ s.)
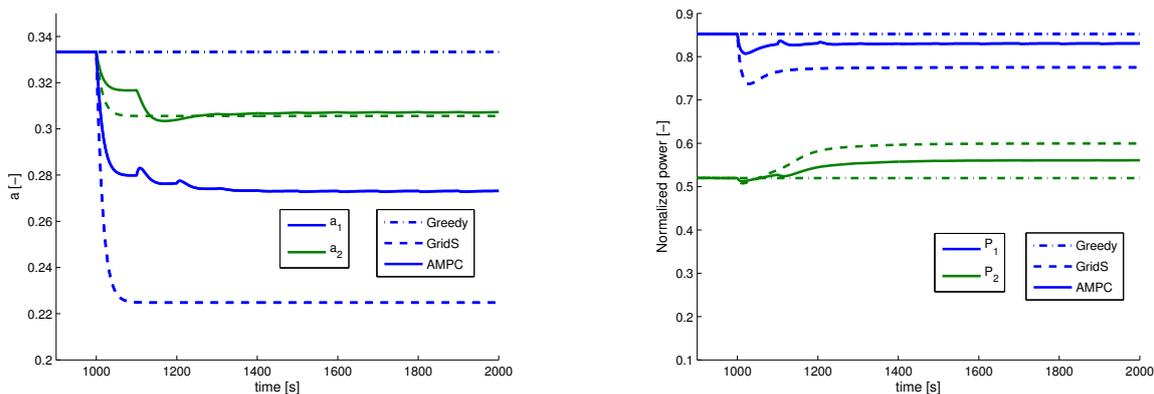

Figure 8: (left) The induction factor, (right) the power production of the individual wind turbines for different simulation cases, with ambient wind $U_\infty = 10$ m/s and yaw misalgnment 10°. The power production is normalized with respect to the total power of the greedy control with fully wake interactions.

Finally, Figure 8 illustrates the time-varying behaviour of the axial induction factor (left) and the corresponding power production (right) of each turbine, for all three control concepts. The noticeable power increases of the downwind turbine (green curves) are referred to the partail wake interactions due to the yaw misalignment. Note that the grid search control settings are obtained for fully wake interactions case study (left image of Fig. 3). Thus, the time-varying atmospheric conditions demand a dynamic closed loop wind farm control. It can be seen that the AMPC regulates the optimal power extraction of the turbines by taking the induced aerodynamic interations of wind turbines into account.

5. Conclusions and future work

A predictive control framework is proposed for optimal energy extraction of wind farms. The optimization problem is constrained to a two dimensional wind farm model. The adjoint method is employed to find the proper search direction with respect to the specified performance index, i.e. the total power of a wind farm at a finite time interval. The optimal solutions are searched at each control horizon, which provides the feedback into the optimization problem. Hence, contrary to the open-loop approaches, the proposed control framework would be able to improve the performance against the time-varying atmospheric or operating conditions. The effectiveness of the AMPC is studied through simulations for two different wind farm operating conditions, compared with the greedy control. Simulation results show that the proposed approach is able to find dynamically the optimal wind turbine control settings. In the future, we evaluate the performance of the AMPC to decrease the wake-induced power-loss and load under time-varying environmental conditions, e.g. wind direction changes and wake meandering. The aeroelastic model of the wind turbine will be included and the control variables will be extended to the practical wind turbine control settings, e.g. pitch, rotor speed and yaw. Furthermore, the computational effort and applicability of the controller will be studied more from practical perspectives.

Acknowledgments

References

[1] Knudsen T, Bak T and Svenstrup M 2015 *Wind Energy* (Wiley Online Library) vol 18 p 1333.
[2] Gebraad PMO, Teeuwisse FW, van Wingerden JW, Fleming PA, Ruben SD, Marden JR and Pao LY 2016 *Wind Energy* (Wiley Online Library) vol 19 p 95.
[3] Marden JR, Ruben SD and Pao LY 2013 *IEEE Transactions on Control System Technology* vol 21 p 1207.
[4] Gebraad PMO, van Wingerden JW 2015 *Wind Energy* (Wiley Online Library) vol 18 p 429.
[5] Johnson K and Fritsch G 2012 *Wind Engineering* vol 36 p 701.
[6] Campagnolo F, Petrović V, Bottasso CL and Croce A 2016 Wind tunnel testing of wake control strategies *Proc. Conf. on American Control Conference* p 513.
[7] Soleimanzadeh M, Wisniewski R and Johnson K 2013 *J. Wind Eng. Ind. Aerodyn.* vol 123 p 88.
[8] Goit JP and Meyers J 2015 *Journal of Fluid Mechanics* vol 768 p 5.
[9] Bewley TR, Moin P and Teman R 2001 *Journal of Fluid Mechanics* vol 447 p 179.
[10] Torres P, van Wingerden JW and Verhaegen M 2011 Modeling of the flow in wind farms for total power optimization *Proc. Conf. on Control and Automation* p 963.
[11] Gebraad PMO and van Wingerden JW 2014 A control-oriented dynamic model for wakes in wind plants *Journal of Physics: Conference Series* vol 524 (0121186).
[12] Annoni J and Seiler P 2015 A low-order model for wind farm control *Proc. Conf. on American Control Conference* p 1721.
[13] Boersma S, Vali M, Kühn M and van Wingerden JW 2016 Quasi linear parameter varying modeling for wind farm control using the 2D Navier-Stokes equations *Proc. Conf. on American Control Conference* p 4409.
[14] Boersma S, Gebraad PMO, Vali M, Doekemeijer BM and van Wingerden JW 2016 A control-oriented dynamic wind farm flow model: "WFSim" *Journal of Physics: Conference Series (in press)*.
[15] Doekemeijer BM, van Wingerden JW, Boersma S and Pao LY 2016 Enhanced kalman filtering for a 2D CFD NS wind farm flow model *Journal of Physics: Conference Series (in press)*.
[16] Versteeg HK and Malalasekera W 2007 *An introduction to computational fluid dynamics: The finite volume method.* Pearson, Prentice Hall.
[17] Bianchi FD, Battista HD and Mantz RJ 2007 *Wind turbine control systems; Principals, Modeling and Gain Scheduling Design.* Springer-Verlag London.
[18] Allgöwer F, Findeisen R and Ebenbauer C 2003 *Control Systems, Robotics and Automation* vol XI.
[19] Roth R and Ulbrich S 2013 *Flow, turbulence and combustion* vol 90 p 763.
[20] Madsen K and Nielsen HB 2010 *Introduction to Optimization and Data Filtering.* DTU Informatics-IMM, Richard Petresens Plads.
[21] Bertsekas DP 2004 *Nonlinear Programming* Athena Scientific.
[22] Knudsen T and Bak T 2013 Simple model for describing and estimating wind turbine dynamic inflow *Proc. Conf. on American Control Conference* p 640.